Microheterogeneous Structure of Local Melted Zones in the Process of Explosive Welding

BELLA A. GREENBERG, MIKHAIL A. IVANOV, ALEXEI V. INOZEMTSEV, ALEXANDER M. PATSELOV, MARK S. PUSHKIN, and ALISA M. VLASOVA

The dispersed structures formed in the process of explosive welding and solidification after melting were investigated in areas near the interface. It was shown that melting can be initiated by particles flying away as a result of granulating fragmentation. This is the fastest process during explosive welding, which is similar to fragmentation in conventional explosions with the formation of fragments but occurring in the presence of a barrier. The reaction between the particles and their environment may lead to local heating sufficient for melting. This is confirmed by the observation of numerous particles of the refractory phase within the local melted zones. In the absence of mutual solubility of the initial phases, the solidified local melted zones are to a certain extent analogous to colloidal solutions of immiscible liquids. Correlations between the typical temperatures were obtained that determine the conditions for the formation of various types of colloidal solutions.

DOI: 10.1007/s11661-015-2968-3

I. INTRODUCTION

THE unusual microstructure of the joints that result from explosive welding is due to the fact that explosive welding is a high-intensity fast process. Typical times: welding process duration about 10^{-6} seconds, deformation rate 10^4 to 10^7 s^{-1}, cooling rate 10^5 K/s. The explosive welding process diagram is shown in Figures 1(a) and (b). Figure 1 shows a schematic of the explosive welding process. Parallel arrangement of the plates was used. A charge of explosive substance was placed on the flyer plate. Existence of the so-called "weldability window" within the impact angle-collision point velocity coordinates (Figure 1(c)) shows the necessary conditions for the formation of a strong joint.[1,2]

The number of joints formed by explosive welding is constantly growing. Moreover, it is possible to obtain joints between metals that have not been obtained using other methods. Explosive welding makes it possible to obtain joints between materials that cannot be obtained by other means, such as steel and titanium, zirconium and steel, and many other materials, on very large areas. Sheets and products of complex shapes can be welded. Both similar and dissimilar metals can be welded. We can obtain quality bi-metal and multilayer composites of high strength.

With all the variety of materials and welding conditions, it is the mixing in the transition zone near the interface that is seen as the central problem. It is the transition zone structure that determines whether adhesion of both materials is possible. Mixing is caused by the effect of a strong external action which involves a massive plastic deformation (including pressure, shear components, turning points of stress, deformation heterogeneity, *etc.*), friction of surfaces, the cumulative jet impact, and other factors.[3] But it remains unclear so far how even with such a strong external action mixing occurs within such a short time period, before the welding process is completed. This question becomes even more critical if we are talking about materials that possess no mutual solubility even in the liquid state.

The role of structural research has been underestimated. As a result some of the stereotypes that earlier were taken for granted have not been confirmed by detailed structural studies. We are talking about conventional views such as the risk of melting, the risk of lack of mutual solubility, and the existence of only one type of fragmentation.

Granulating fragmentation (GF) is a process of segmenting into particles which either fly away or couple with each other. In other words, GF includes both formation and flying away of the particles and their partial consolidation. In both cases—both in case of a normal explosion and in case of GF—flying away of particles (fragments) is observed, but continuity of materials is only preserved in case of GF. Unlike fragmentation in the process of the explosion, GF

BELLA A. GREENBERG, Professor, ALEXEI V. INOZEMTSEV and ALEXANDER M. PATSELOV, Senior Researchers, and MARK S. PUSHKIN, Postgraduate, are with the Physics of Deformation Department, M.N. Miheev Institute of Metal Physics, Ural Branch, Russian Academy of Sciences, S. Kovalevskaya Str. 18, Ekaterinburg 620990, Russia. Contact e-mail: bella@imp.uran.ru MIKHAIL A. IVANOV, Professor, is with the Department of Theory of Nonideal Crystals, Kurdyumov Institute of Metal Physics, National Academy of Sciences of Ukraine, Vernadskogo Blvd. 36, Kiev 03680, Ukraine. ALISA M. VLASOVA, is Senior Researcher with the Physics of Deformation Department, M.N.Miheev Institute of Metal Physics, Ural Branch, Russian Academy of Sciences, and also Assistant with the Ural Federal University named after the first President of Russia B.N. Yeltsin, Mira Str. 19, Ekaterinburg 620002, Russia.
Manuscript submitted January 29, 2015.
Article published online May 27, 2015

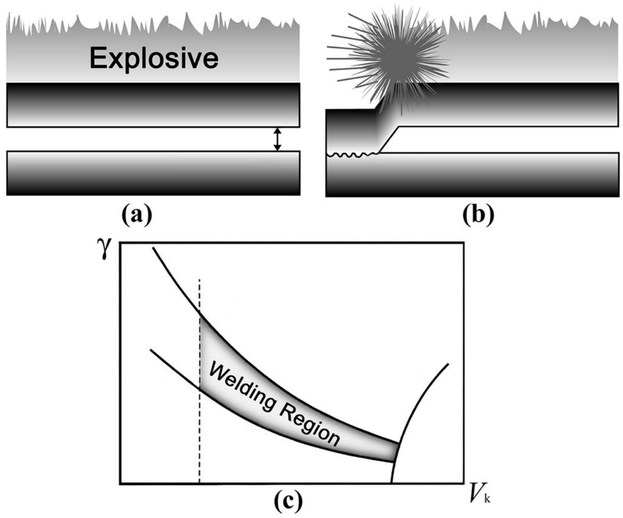

Fig. 1—(*a*, *b*) Schematic diagram for obtaining bimetallic joints by explosive welding; (*c*) "weldability window".

occurs in the presence of the barrier, in particular, the second plate (not the one from which the particles are emitted). Particles (fragments) are stopped by the barrier in any case, and flying away of solid particles in the refractory phase can provoke melting of the lower melting point phase.

This paper proposes a new concept for solidified local melted zones being filled with dispersed particles, *i.e.*, for the occurrence of colloidal solution analogs. The proposed approach allows us to understand and consistently explain the experimental facts collected in their totality. The sequence of the sections of this work corresponds to the internal logic of the proposed approach: Part II (Materials and joints) is followed by a summary of the processes in explosive welding. Section III begins with the most rapid process. This GF is analogous to fragmentation resulting from an explosion. It is GF that causes local melting which is discussed in Section IV. The following scenario is possible: local flying away of particles (fragments), local melting, and preservation of the fragmented layer of the particles that have failed to fly away. In Section V, methods of the fractal theory are used mostly to describe the suspensions that fill the local melted zones. For the first time, the article provides data to prove self-similarity of tantalum particles in these areas. Section VI covers relation between typical temperatures that corresponds to the filling of the local melted zones with suspensions. Finally, Section VII focuses on one of the most successful implementations of explosive welding. Based on this study, it became possible to identify the reasons for the high quality and stability of a chemical reactor with walls containing a Cu-Ta joint with a wavy interface and dispersion-hardened local melted zones.

II. MATERIALS AND JOINTS

The study mainly uses experimental results obtained for the copper-tantalum joints with both flat and wavy interfaces and also results for some other joints for comparison.[4,5] For convenience, the following notations that were introduced for the joints earlier are used here: ($\mathbf{A}_w$)—titanium-orthorhombic titanium aluminide (hereinafter, for short, aluminide); ($\mathbf{C}_p$), ($\mathbf{C}_w$)—copper-tantalum; ($\mathbf{D}_w$)—iron-silver; ($\mathbf{E}_p$)—aluminum-tantalum. The subscript corresponds to the following interface shape: p—flat, w—wavy).

Figures 1(a) and (b) show the explosive welding process. When the ($\mathbf{A}_w$) titanium-orthorhombic titanium-aluminide joint was welded, an indent was made in the bottom titanium plate (base plate) where an orthorhombic titanium alloy sheet was placed and fixed. An explosive substance charge was placed on the top (cladding) titanium plate. During its explosion, the velocity of the plate reached 500 m/s and the collision angle was 12 to 14 deg. During detonation of explosive, the pressure developed on the contact surface was ~6 GPa and the material adjacent to the contact surface was heated to ~1173 K (900 °C) and underwent plastic deformation of 40 to 80 pct.

We will limit ourselves to showing here only the key welding parameters for the test joints

$$(\mathbf{C}_p):\gamma = 5.22\,\text{deg},\ V_c = 2680\,\text{m/s},\ V_i = 234\,\text{m/s};$$

$$(\mathbf{C}_w):\gamma = 11.8\,\text{deg},\ V_c = 2125\,\text{m/s},\ V_i = 440\,\text{m/s};$$

$$(\mathbf{A}_w):\gamma = 13\,\text{deg},\ V_c = 2200\,\text{m/s},\ V_i = 500\,\text{m/s};$$

$$(\mathbf{D}_w):\gamma = 15.6\,\text{deg},\ V_c = 1910\,\text{m/s},\ V_i = 520\,\text{m/s};$$

$$(\mathbf{E}_p):\gamma = 8.6\,\text{deg},\ V_c = 2000\,\text{m/s},\ V_i = 300\,\text{m/s},$$

where γ is collision angle, V_c is collision velocity, and V_i is impact velocity.

Experimental studies of the microstructure were carried out using the following methods: X-ray diffraction analysis (DRON-3), scanning and transmission electron microscopy (JEM200CX and SM-30 Super Twin electron microscopes, QUANTA 200 FEI Company and Quanta 600 scanning electron microscope; and Fashione 1010 ION MILL ion gun).

Difficulty in making foils out of dissimilar materials is the reason for insufficient development of electron microscopic research of welded joints. In the process of thinning, one of the metals may be completely etched out, so that only the foil from another material is left. Thus, for the copper-tantalum joints, given the high corrosion resistance of tantalum, etching of copper can only be prevented by special selection of reagents. The use of an ion gun is the most efficient method.

Next, results of electron microscopic observation of the structure, including the interface shape, the surface roughness, flying away of particles in the melted zone, the intensive deformation area, *etc.* are shown.

III. FRAGMENTATION

Fragmentation is a long-known phenomenon. It is observed in biology, genetics, medicine, geology, and in many other areas. For example, fragmentation of algae and primitive worms as their method of reproduction, fragmentation of corals that leads to the formation of reefs, *etc*. It is fragmentation during explosion that is relevant to the processes that are discussed in this paper. Such fragmentation is a process of segmentation (partitioning) of a solid body into pieces (fragments) that occurs under strong external influence. Hence the names: *fragmentation warhead, fragmentation shell, fragmentation bomb*. Description of the fragment fly away process is usually attributed to Neville Mott.[6] Together with other authors (see, for instance, the book by Grady[7]), he developed the theory of dynamic fragmentation in case of an explosion.

Despite the vast variety of welded joints, there are not so many processes that control their formation. First of all, it is a new type of fragmentation discovered by the authors of this paper and was named GF.[8] It is similar to the fragmentation in the process of explosion studied by Mott. We believe that the fragments scatter during explosion that was studied by Mott and flying away of particles in explosive welding have much in common. However, the scatter of fragments in the explosion occurs in open space, whereas in case of explosive welding, particles fly away in a closed space between the plates. This means that in the case of explosive welding, fragmentation is constrained. In the case of welding, the role of explosion consists in acceleration of one body relative to another, so that most of the chemical energy of the explosive is transformed into kinetic energy of the flyer plate which is transformed into other forms of energy in case of collision.

Figure 2 shows various stages of GF for the ($\mathbf{A}_w$) joint titanium-orthorhombic titanium aluminide.[9–11] The welding parameters for this joint are shown in Section II above. The choice of such joint was determined by the following factors. Obtaining metal-intermetallic joints is one of the most difficult problems in welding. We have tried to use explosive welding to solve this problem. The attempt was successful, perhaps due to the fact that this type of welding is quick and diffusion free. Due to the peculiarities of phase transformations of orthorhombic titanium aluminide, the authors were able to obtain its joint with titanium, while titanium joints with other titanium aluminides have not been obtained.

In Figure 2 titanium aluminide is clearly visible because of the globules α_2-phase (structure $D0_{19}$). GF occurs on the surface of aluminide. Hence the flying away of particles and the formation of a melted zone in the adjacent titanium plate containing aluminide particles occur. A layer of particles that failed to fly away remains on the surface.

Flying away of micron particles of aluminide which is clearly seen in Figures 2(a) and (b) is remarkably similar to scattering of fragments in case of an explosion, only the sizes are different. But in case of an explosion the fragments scatter in open areas, whereas in case of explosive welding the particles fly away in a closed space between the plates. The high magnification image in Figure 2(c) shows a fragmented layer consisting of aluminide particles. Figure 2(d) shows clearly visible particles of titanium aluminide in the local melted zone with dimensions varying within the range of 100-500 nm. Numerous particles within the local melted zones can be observed for other joints as well, including tantalum nanoparticles in copper (flat interface), micron particles of tantalum in copper (wavy interface), micron particles of iron in silver (wavy interface), *etc*.[12]

Unlike the process of fragmentation, in the process of explosion resulting in destruction that was studied by Mott, GF occurs as a result of microfracture and is a process alternative to fracture. Instead of free surfaces, the occurrence of which would lead to fracture, surfaces associated with the microfracture are formed. These are either part of the flying away particles or are ‘‘healed'' in the process of their consolidation. Microcracks do not occur under the influence of medium-applied stress but rather on its local concentrators. It is in areas containing local concentrators of stress that many microcracks may occur. The relevant free surfaces slow down when ‘‘meeting'' each other. First, this prevents transformation of microcracks into macrocracks. Secondly, microvolumes surrounded by free surfaces on all sides occur. The said microvolumes are actually cut out of the surrounding material. GF increases ‘‘survivability'' of material, saving it from destruction, even in the case of such a strong external impact as explosive welding. This is the essential role of GF in case of explosive welding.

Among the set of the joints examined, there were no occasions where fragmentation was not found. This means that GF is a universal phenomenon which is inherent to explosive welding.

GF is a fast process that proceeds in the explosion time. In addition to GF, another type of fragmentation that usually occurs in the cases of intensive deformation, is also observed in the process of explosive welding.[8] Such fragmentation which can be called traditional includes pumping of dislocations, formation of various kinds of structures, recrystallization, and other processes. For the ($\mathbf{D}_w$) iron-silver joint Figure 3 shows cellular, banded, and recrystallized structures which are observed in silver. Similar structures are observed in iron.

Both types of fragmentation are easily distinguishable: in case of conventional fragmentation, neither particles fly away nor melting occurs. In contrast to GF which is observed in close vicinity of the interface, traditional fragmentation occurs at a slightly greater distance from it.

IV. LOCAL MELTING

GF is analogous to the fragmentation in the explosion but occurs in the presence of strong barriers. For particles flying away from one plate during explosive welding, such barriers that stop them will include the second plate, and the remaining bulk of the original plate. One can assume that flying away of the solid particles of the phase that does not melt will initiate local melting of the material with a lower melting point near the interface. The reason is that due to the large total area of the particles, effective friction between particles and the barrier may cause local heating sufficient for melting. To some extent these flying

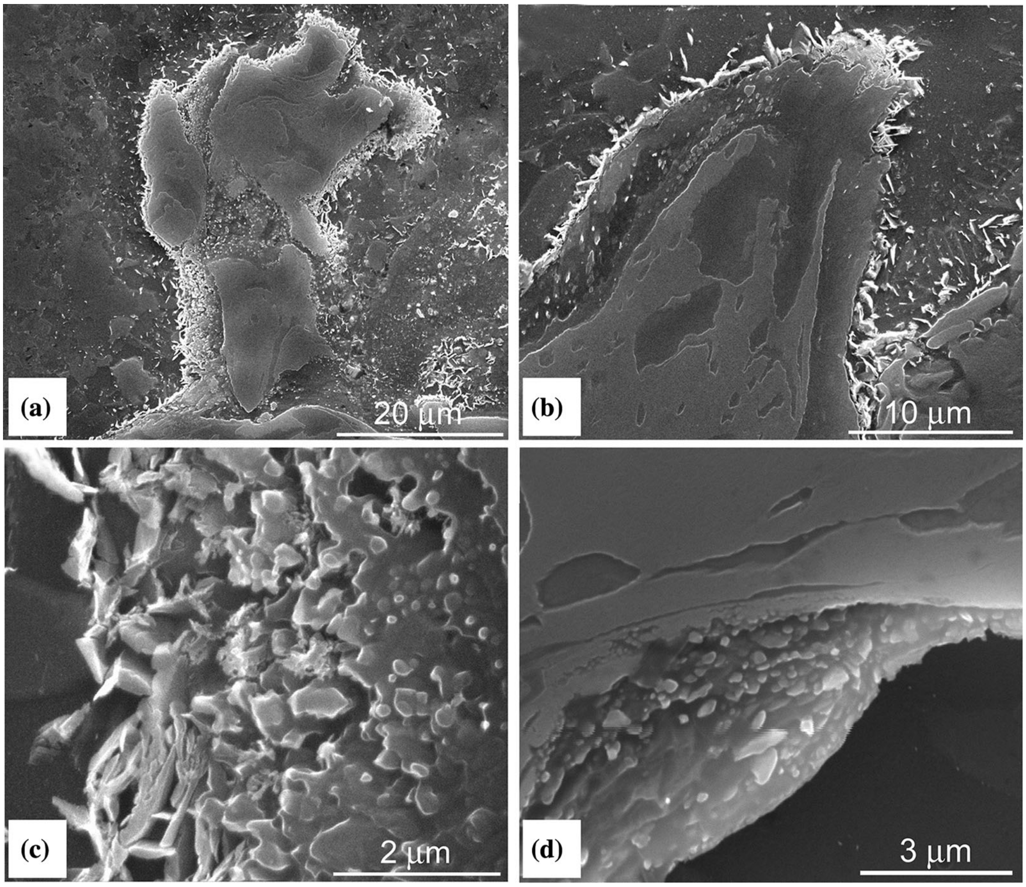

Fig. 2—($\mathbf{A_w}$) titanium-aluminide joint, granulating fragmentation: (*a*, *b*) flying away of aluminide particles; (*c*) fragmented aluminide layer; (*d*) aluminide particles inside the local melted zone.

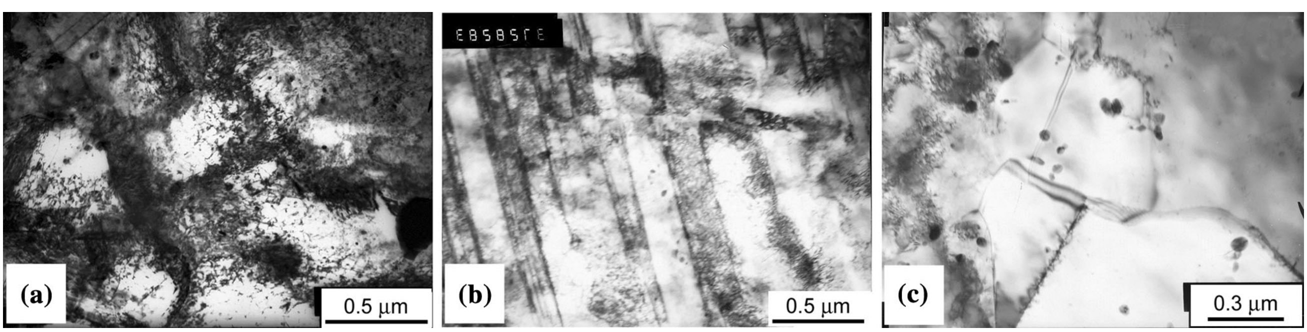

Fig. 3—($\mathbf{D_w}$) iron-silver joint, silver fragmentation during intensive plastic deformation: (*a*) cellular structure; (*b*) band structure; (*c*) recrystallized structure.

particles are analogs of sparks that can frequently be observed in the situation of strong dry friction between materials.

In the case of explosive welding, this mechanism works regardless of whether or not the initial phases possess mutual solubility. In case of immiscible phases, its action may result in the microheterogeneous structure in the local melting zones.

Figure 2(d) illustrates the relation between flying away of aluminide particles and local melting of titanium for the ($\mathbf{A_w}$) joint. In this case, numerous aluminide particles are embedded in the solid solution of titanium alloyed with niobium and aluminum that are originally part of aluminide.

Thus, the following scenario is possible: local flying away of particles (fragments), local melting, and preservation of the fragmented layer of the particles that have failed to fly away. The shape of particles within the local melted zone for the ($\mathbf{A_w}$) titanium-aluminide joint is clearly visible in Figure 2(d). The question remains why the fragment type particles inside the area that was previously melted are rather smooth. Indeed, in Figure 2(c), the fragmented layer contains not only smooth but also indented particles. It is but natural to assume

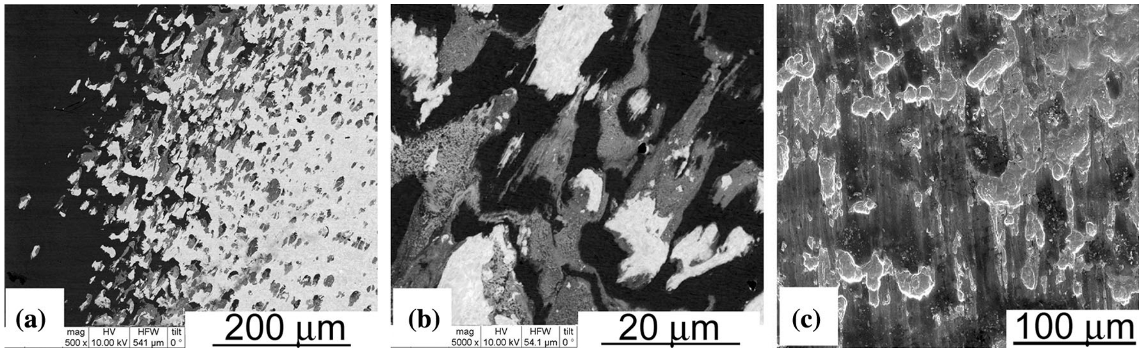

Fig. 4—Flat interface, longitudinal section (SEM): (*a*, *b*) (**C**$_p$) copper-tantalum, at different magnifications; (*c*) (**E**$_p$) aluminum-tantalum; white—tantalum, black—copper (aluminum), gray—melted zones.

that the fly away of smooth particles is an easier process than that of indented ones. Therefore smooth (or rather, less indented) particles fly away, while the indented ones remain on the edge of the refractory phase.

Figures 4(a) and (b) show the SEM image of a longitudinal section of the transition zone for the (**C**$_p$) copper-tantalum joint.[13] White, black, and gray spots are visible. The tricolor structure of the longitudinal cross section is due to the cusps on the interface. In the presence of cusps, their intersection with the plane parallel to the interface would result in areas containing different metals being observed simultaneously; therefore, the image would be bicolor. However, Figures 4(a) and (b) show three rather than two areas. In addition to the areas filled with base metals, there is a gray local melted zone containing a mixture of both metals.

As a result, the interface will have a chaotic topography with a large number of cusps and cavities. The same tricolor image of a longitudinal section is shown in Figure 4(c) for the (**E**$_p$) aluminum-tantalum joint.[14] This means that the tricolor type of longitudinal section for the flat interface is observed regardless of whether the base metals possess mutual solubility (such as aluminum-tantalum) or do not possess it (such as copper-tantalum).

Figure 5 illustrates the scenario of how particles are formed, particles of one type fly away and others become partially consolidated for the (**C**$_w$) copper-tantalum joint with wavy interface. Figure 5(a) shows alternating bands of copper and tantalum. Note the large tantalum cusp (Figure 5b). A local melted zone can be seen on the next copper band. The remaining tantalum particles that did not fly away before the process was completed are clearly visible in Figure 5(c). The microheterogeneous structure of the local melted zone for the same (**C**$_w$) joint is shown in Figure 6(a). Micron particles of tantalum are visible. They are rather smooth and elongate. At the same time the fragmented layer (Figure 5(c)) comprises mainly indented islands. Thus there is complete analogy with the situation discussed above for (**A**$_w$) titanium-aluminide joints with indented particles within the fragmented layer and smooth and elongated ones in the melted zone.

The microheterogeneous structure of the local melted zone for the (**C**$_p$) joint is clearly visible both in the SEM (Figure 6(b)) and the TEM images (Figure 7). Figure 7(a) shows a bright-field image of the microstructure of the local melted zone. Figure 7(c) shows the corresponding dark-field image obtained in reflection $\langle 111 \rangle$ Cu, and Figure 7(d) represents the dark-field image obtained in reflection $\langle 110 \rangle$ Ta. In Figure 7 the tantalum particles are dark. In the diffraction pattern (Figure 7b) a ring system consisting of individual reflections, belonging to tantalum, is observed. The strong point reflections belong to copper.

The difference in size and distribution of the dispersed phase particles leads naturally to different values of microhardness measured in the local melted zones. For the (**C**$_p$) joint with the highest density of tantalum particles, microhardness in the said zone is about 4000 MPa, which is 1000 MPa higher than microhardness of tantalum and 3000 MPa higher than that of copper. However, for (**C**$_w$) joint microhardness in the said zone is almost the same as microhardness of tantalum. As shown by mechanical tests, the shear strength is also higher for the (**C**$_p$) joint and is approximately 230 to 240 MPa, while for the (**C**$_w$) joint it is about 150 to 170 MPa, which, nevertheless, is still greater than the strength of copper.

V. FRACTAL DESCRIPTION OF INTERFACES

The search of fractals within the transition zone of the joints formed by explosive welding was initiated after the observation of numerous objects that give the impression of being self-similar.[15] These include cusps, dendrites, solid phase particles within the local melted zones, *etc*.

Heterogeneity of the interface is in fact three dimensional. At the same time, the observed electron microscopic images show a set of two-dimensional sections of the interface. The longitudinal cross sections of both the cusps and the local melted zones are basically islands surrounded by other phases. Although the particles within the local melted zones have a different origin, they also appear as islands. Islands of different types are probable fractal objects, which are analyzed in this section. Interpenetration of different materials in the process of explosive welding makes emergence of islands

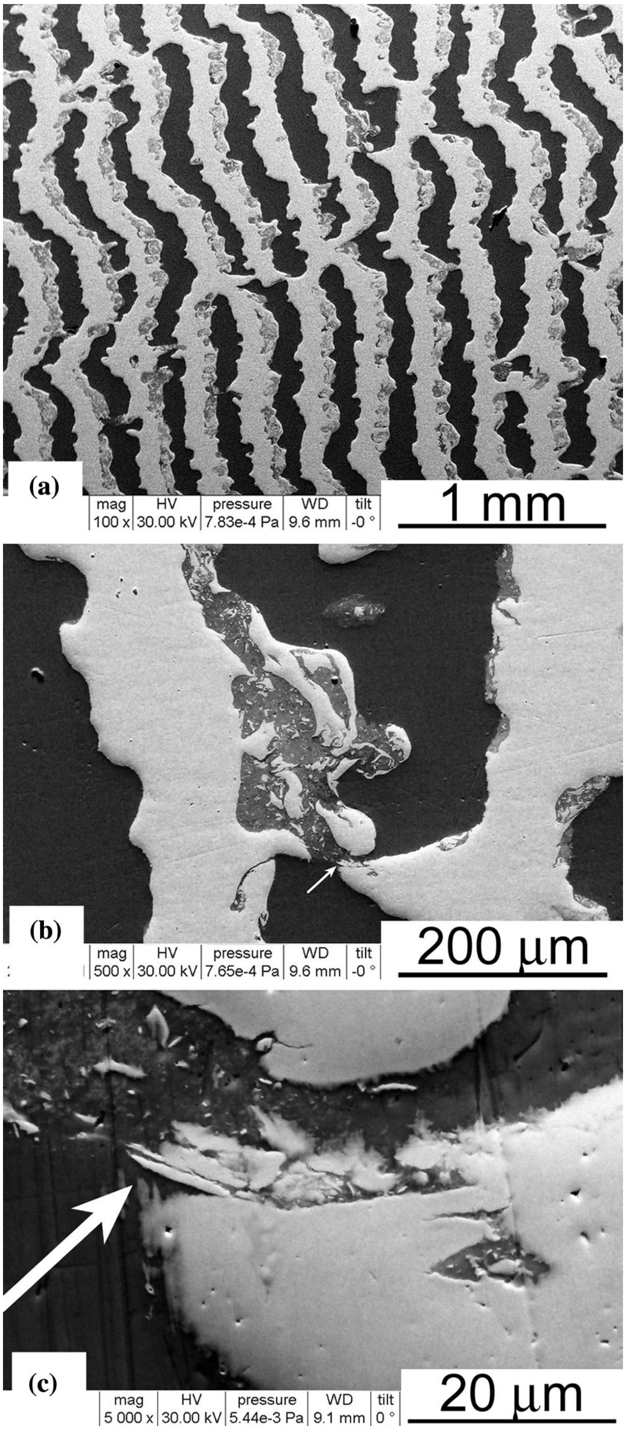

Fig. 5—($\mathbf{C}_w$) copper-tantalum joint, longitudinal cross section: (*a*) copper and tantalum bands; (*b*) large cusp and local melted zone; (*c*) remaining tantalum particles.

of different colors inevitable, which is typical for the structure of welded joints.

Formation of cusps resulting from diffusionless emission of one metal into the other in the process of welding is a typical stochastic process. It is the nature of the process described above along with the observations that indicate recurrence of the structures that encourages development of the fractal approach to describe the topography of the interface.

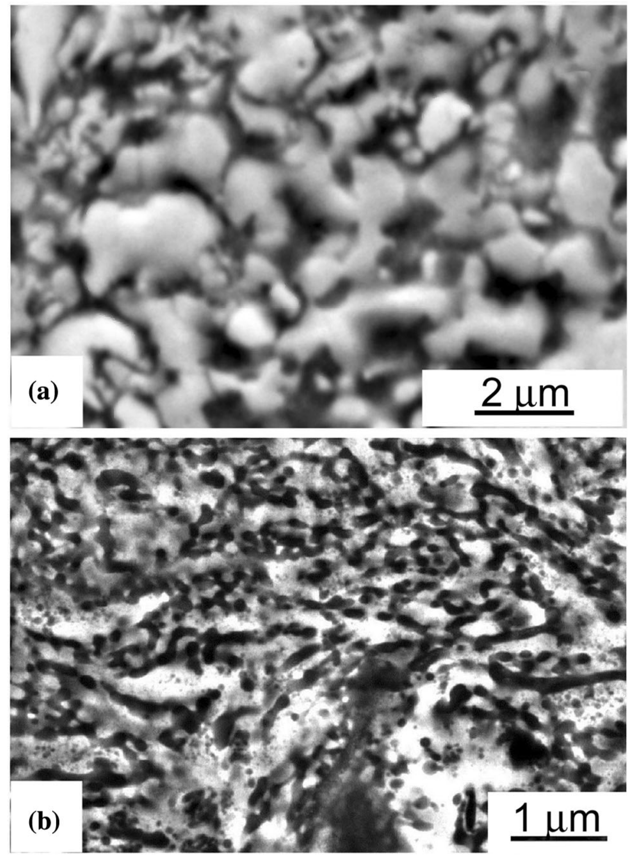

Fig. 6—Microheterogeneous structure of melted zones for tantalum-copper joints, longitudinal section (SEM): (*a*) ($\mathbf{C}_w$) joint; (*b*) ($\mathbf{C}_p$) joint.

The tricolor image shown in Figure 4(a) was transformed as follows. First, we kept only longitudinal sections of tantalum cusps—the white islands. Their environment included the areas filled with copper and the local melted zones. The environment of the white islands was considered to be the black background. The set of white islands for the ($\mathbf{C}_p$) joint obtained in this manner and investigated further is shown in Figure 8(a). Likewise, the gray islands against the black background were obtained for the same ($\mathbf{C}_p$) joint (Figure 8(b)).

In order to find out whether the islands are fractal objects, it is necessary to obtain the ratio between the perimeter of each of the islands and its area. We will calculate the dimensions of the islands using the methods utilized in the theory of fractals.[16,17] Mandelbrot[16] showed that the islands with the outlines which are to some extent similar satisfy the following ratio between their perimeters $L(\delta)$ and areas $A(\delta)$:

$$L(\delta) = C\delta^{(1-D)}[A(\delta)]^{D/2}, \qquad [1]$$

where D is the fractal dimension and δ is the selected length benchmark. With certain approximations of (1) we obtain the simple proportionality ratio which looks as follows:

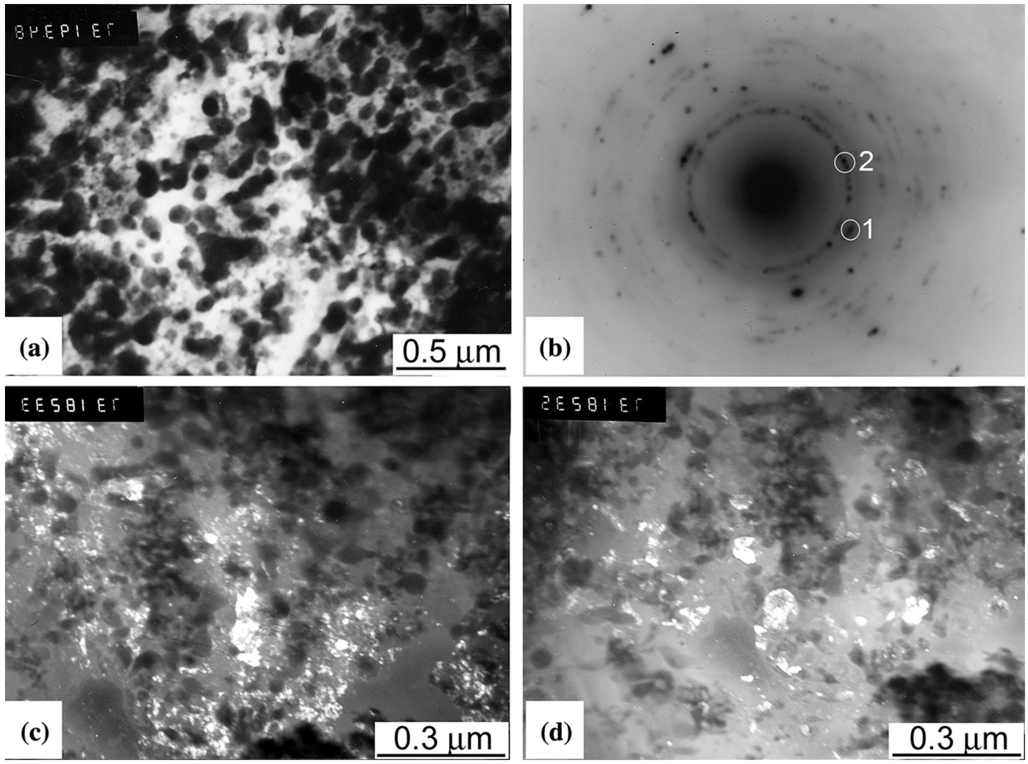

Fig. 7—Microheterogeneous structure of melted zones for ($\mathbf{C}_p$) joint, longitudinal section (TEM): (*a*) bright-field image; (*b*) microdiffraction; (*c*) dark-field image (a) obtained in reflection $\langle 111 \rangle$ Cu, (*d*) dark-field image (a) obtained in reflection $\langle 110 \rangle$ Ta.

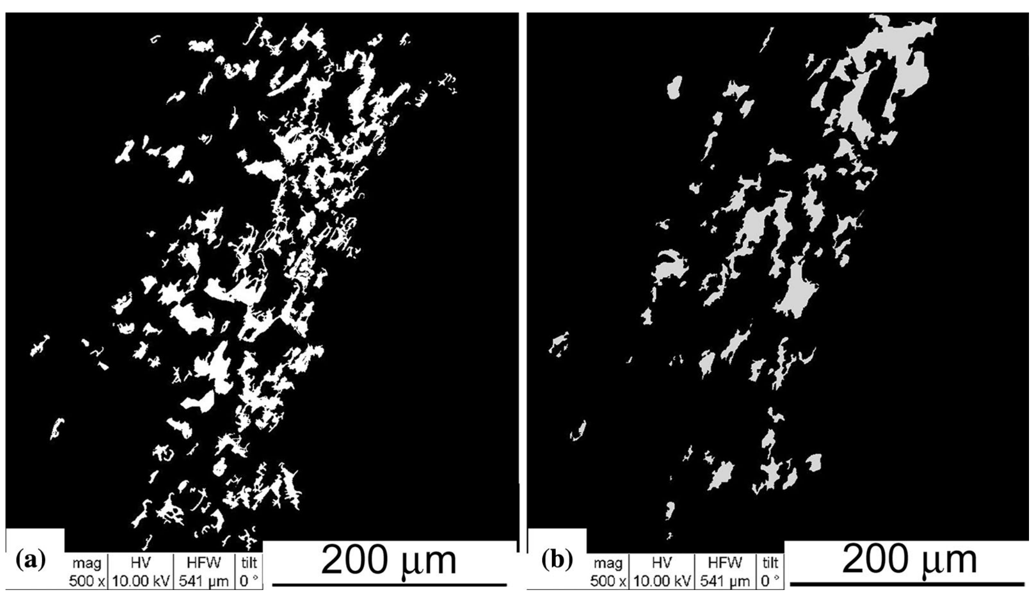

Fig. 8—($\mathbf{C}_p$) joint, longitudinal cross section: (*a*) white islands; (*b*) gray islands.

$$A \sim L^{2/D}, \quad \log A \sim \frac{2}{D} \log L \qquad [2]$$

For each of the islands shown in Figure 8, area A and perimeter L were calculated and then applied to the graphical image within the $\log A$ from $\log L$. In this case, each island is a single point. Next, an approximating line is found for each type of islands as shown for example in Figure 9, and the tangent of the slope angle of this line which, according to [2], is equal to $2/D$, is used to calculate the value of fractal dimension D for the given set of islands. The fact that the dimension measurements for the set of islands of the same type are placed on the same line is, to a certain extent, the evidence of their fractal nature. Approximating lines for different types of islands in the main part are shown in Figure 9.

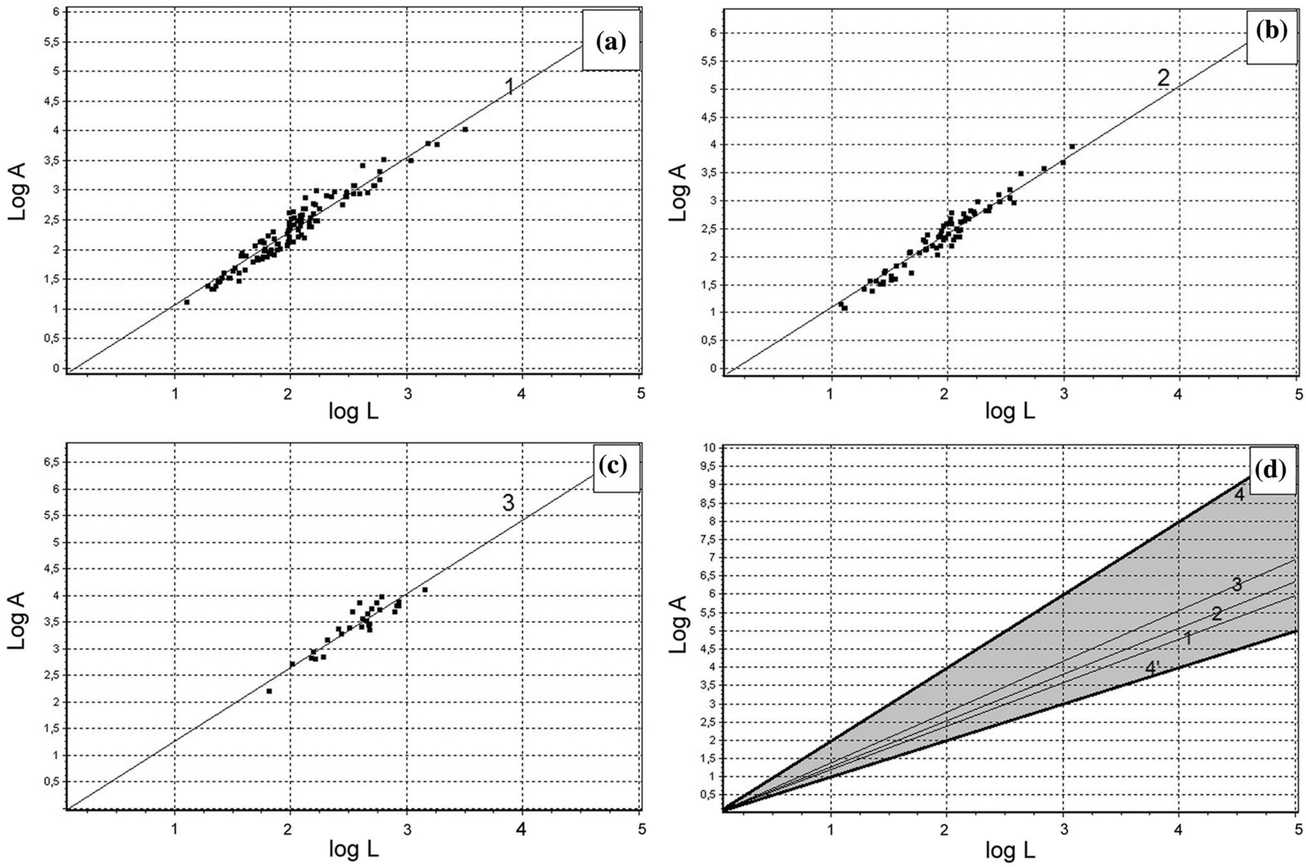

Fig. 9—Relation of the area to the island perimeter; (*a*) line 1—gray island, ($\mathbf{C}_p$) joint; (*b*) line 2—tantalum islands within the melted zone for ($\mathbf{C}_p$) joint; (*c*) line 3—tantalum islands within the melted zone for ($\mathbf{C}_p$) joint; (*d*) 4—round islands ($D_4 = 1$); 4′— limit for two-dimensional objects ($D_{4'} = 2$).

Line 1, just like in Figure 9(a), pertains to the gray islands are shown in Figure 8(b) for ($\mathbf{C}_p$) joint. Lines 2 and 3 represent the tantalum islands within the melted zone for the ($\mathbf{C}_p$) joint (Figures 6(b) and 7), and ($\mathbf{C}_w$) joint (Figure 6(a)), respectively. Straight line 4 represents the area-perimeter correspondence for round islands when the D parameter has the lowest value $D_4 = 1$. Figure 9(d) shows line 4′, which corresponds to the maximum dimension for two-dimensional fractal objects $D_{4'} = 2$.

We therefore obtain the following values, for D parameters corresponding to lines 1, 2, and 3: $D_1 = 1.58 \pm 0.06$, $D_2 = 1.44 \pm 0.03$, $D_3 = 1.22 \pm 0.09$.

As can be seen from the comparison of lines 1 to 3 with line 4, if the area A value is fixed, the corresponding value of perimeter L is lower for round islands. This means dimensions can be increased through irregularity of the islands. As seen from the comparison in Figures 8(a) and (b), the gray islands are less indented than the white ones. This is due to the fact that they can spread out before they are solidified. Indeed, the D_1 dimension of the gray islands is significantly smaller than one of the white tantalum islands which is equal to (1.68 ± 0.07). The high irregularity of the cusps and therefore the islands of tantalum with the largest dimension out of those calculated in this paper help cusps serve as “wedges” connecting contact materials with the highest effect.

The tantalum particles within the local melted areas are significantly different for ($\mathbf{C}_p$) and ($\mathbf{C}_w$) joints. As seen from Figures 6(b) and 7, for the ($\mathbf{C}_p$) joint these are nanoislands approximately 30 to 50 nm in size. For the ($\mathbf{C}_w$) joint these are micron islands (Figure 6(a)). From the comparison of images it can be seen that the micron islands are much smoother. The value D_3 of the corresponding dimension is the lowest of those obtained for the joints studied in this paper.

We believe that in the general case, the convex shape of the islands reduces their fractal dimensions, while the presence of concave segments in the outlines of the island, on the contrary, increases them. For ($\mathbf{A}_w$) titanium-aluminide joint, Figure 2(d) shows the image of a local melted zone containing aluminide particles and Figure 2(c) shows the image of the fragmented layer of particles that fail to fly away. For the islands within the local melting area the dimension is approximately 1.32 ± 0.09, while for the islands within the fragmented layer the dimension is approximately 1.49 ± 0.08.

Thus, the ideas developed above that, firstly, the indented particles have greater dimensions in comparison to the smooth ones, and secondly, that the smooth particles fly away more easily than the indented ones, are fully confirmed.

The "smooth *vs* indented" contradistinction provides a purely qualitative description of the surface state. Fractal dimensions provide a quantitative characteristic that allows to take into account both the area and perimeter of the investigated elements of the interface and their changes with welding conditions or passing from one welded joint to another.

VI. RELATIONS BETWEEN TYPICAL TEMPERATURES

Next, we consider the conditions under which certain types of microheterogeneous systems are formed near the interface in melts solidified after explosive welding or, otherwise, where solidified colloidal solutions are formed.[18] We will at first limit ourselves to the case where no boiling of any of the materials occurs during explosive welding and, accordingly, no gas phase is formed. What is essential in this case is the ratio between the following temperatures:

$T_m^{(I)}$—melting point of metal I,
$T_m^{(II)}$—melting point of metal II,
T_s—The temperature near the interface.

We assume for the sake of certainty that $T_{\mathrm{m}}^{(\mathrm{I})} > T_{\mathrm{m}}^{(\mathrm{II})}$ and begin by considering the case where

$$T_{\mathrm{m}}^{(\mathrm{I})} > T_{\mathrm{s}} > T_{\mathrm{m}}^{(\mathrm{II})} \qquad [3]$$

Formula [3] describes the situation shown in Figures 2 and 4: melt of fusible phase II containing solid particles of refractory phase I is formed in the welding process. The refractory phase is made up of either orthorhombic titanium aluminide (joint (**A**$_\mathbf{w}$)) or tantalum ((**C**$_\mathbf{w}$) joint).

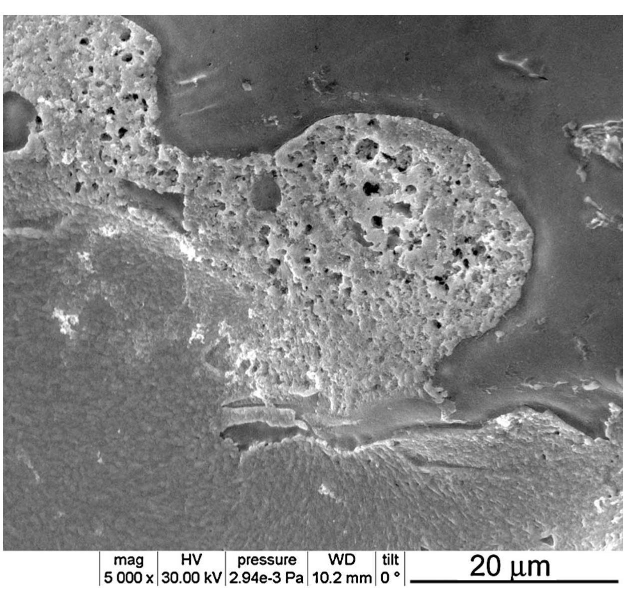

Fig. 10—(**D**$_\mathrm{w}$) iron-silver joint, longitudinal sectional SEM: iron particles in silver.

Reasons for the meltdown of one of the phases caused by friction between particles of the refractory phase and the barrier were discussed above.

In this case, circulation in the liquid phase causes mixing of the colloidal solution which becomes a solidified suspension that is dispersion strengthened due to the presence of the refractory phase particles.

We now consider the case when

$$T_{\mathrm{s}} > T_{\mathrm{m}}^{(\mathrm{I})} > T_{\mathrm{m}}^{(\mathrm{II})} \qquad [4]$$

This means that within the $T_{\mathrm{s}} > T > T_{\mathrm{m}}^{(1)}$ temperature range both metals are melted. In this case a strong external impact leads to both liquids being broken into droplets, so that an emulsion-type colloidal solution is formed. However, the emulsion is in fact unstable, meaning that the droplets of the same sort coalesce and separation into two immiscible liquids is likely. Such separation is, in any case, does not occur for the so-called diluted emulsion where the concentration of one phase is considerably lower than that of the other.

Alternatively, when the condition

$$T_{\mathrm{m}}^{(\mathrm{I})} > T_{\mathrm{m}}^{(\mathrm{II})} > T_{\mathrm{s}} \qquad [5]$$

is satisfied, both metals do not melt during welding and no colloidal solutions are formed.

Thus, either emulsion or suspension is formed in case of colloidal solutions of immiscible liquids that are solidified after welding. When emulsion is solidified, it poses risk to continuity of the joint due to possible separation, while suspension, on the contrary, can contribute to strengthening the joint.

For copper-tantalum and iron-silver joints, typical temperatures are approximately the following: $T_{\mathrm{m}}^{(\mathrm{Ta})} = 3269$ K (2996 °C); $T_{\mathrm{m}}^{(\mathrm{Cu})} = 1357$ K (1084 °C); $T_{\mathrm{m}}^{(\mathrm{Fe})} = 1812$ K (1539 °C); $T_{\mathrm{m}}^{(\mathrm{Ag})} = 1235$ K (962 °C). Let us assume that the temperature is near the interface $T_{\mathrm{s}} = 1500$ K to 1700 K (1227 °C to 1427 °C). Then, for both systems, ratio [3] applies and dispersion strengthened suspension is formed. If, however, $T_{\mathrm{S}} = 2000$ K (1727 °C), then ratio [3] still applies for (**C**$_\mathrm{p}$), (**C**$_\mathrm{w}$) copper-tantalum joints and suspension is formed, while ratio [4] applies in case of (**D**$_\mathrm{w}$) iron-silver joints and emulsion is formed.

For (**D**$_\mathrm{w}$) iron-silver joint, the local melted zone consists of silver containing iron particles (Figure 10). It is essential that the local melting structure is heterogeneous: there are areas where the iron particles are almost invisible. This means that concentrated and weak solutions of iron are simultaneously present in silver. However, no separation of the (**D**$_\mathrm{w}$) iron-silver joint was observed.[19]

Explosive welding may lead to the formation not only of emulsions and suspensions but also another form of colloidal solutions, namely foam.[18] It can be expected that foam will be formed on the interface for immiscible phases at a certain ratio of typical temperatures. Let us assume that relation [4] applies so that both metals are melted near the interface. If additionally the relation

$$T_{\mathrm{s}} > T_{\mathrm{b}}^{(\mathrm{II})} \qquad [6]$$

applies in the case of low-melting metal with the boiling temperature $T_b^{(II)}$, then formation of foam near the interface is likely.

In this regard, consider the joint resulting from explosive welding of magnesium-titanium metals possessing limited solubility. Characteristic temperatures have following values: $T_m^{(Ti)} = 1941$ K (1668 °C), $T_m^{(Mg)} = 923$ K (650 °C), $T_b^{(Mg)} = 1368$ K (1095 °C). Due to the low boiling temperature, magnesium melt may contain the gas phase in addition to other phases. It is considered an established fact that formation of stable foam is totally impossible in pure liquid. However, it is believed that in those areas where both metals are melted, formation of foam is likely in which layers of liquid are formed by magnesium-titanium colloidal solution and the bubbles are filled with magnesium vapors. Whipping or shaking of the liquid is also required for foam formation, which naturally happens in the process of explosion. Due to rapid quenching after the explosion action, liquid dispersion medium turns into solid phase medium and the dispersed gas phase is preserved. The result is high stability of solid foam. This also means that pores will occur and be observed in the vicinity of the interface. Figure 11 shows two welded titanium-magnesium joints obtained in different modes of explosive welding: (a) $\gamma = 21.5$ deg, $V_c = 2000$ m/s, $V_i = 740$ m/s; (b) $\gamma = 21.5$ deg, $V_c = 2300$ m/s, $V_i = 860$ m/s. In case (a), the interface is flat, in case (b) it is wavy. As seen from Figure 11, the state of the interfaces is also different in these cases: in contrast to the dense interface in mode (a), in case (b) the interface is porous. Pores are clearly visible in Figure 12.

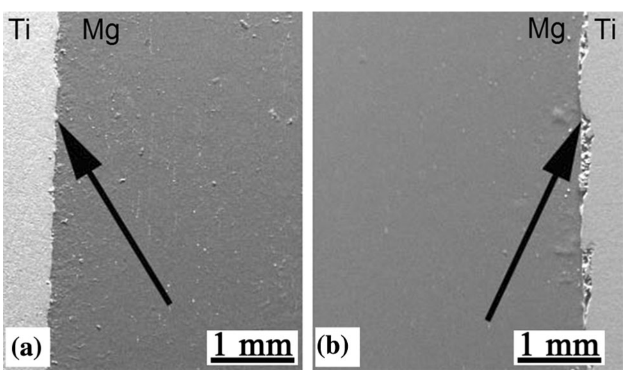

Fig. 11—Magnesium-titanium: (*a*) dense interface; (*b*) porous interface.

We note here that pure magnesium is unsuitable for welded structures due to its low corrosion resistance and low strength. Therefore magnesium alloys are used as structural material. Of all the structural materials, magnesium alloys have the lowest density (4 times lower than steel), which makes them suitable for use in structures in which weight is the main parameter.[20] However, when designing composites as aerospace materials one should bear in mind the likelihood of magnesium boiling in the process of explosive welding.

VII. MELTING AND RISK ZONES

It is known[21] that for many materials, such as polymers, solution or melt of the material is considered to be the best adhesive. This to some extent proves that bonding of the metals under study is also possible due to their melting during explosive welding. Indeed, melting helps simultaneously solve problems of wetting, adhesion, thermal expansion, and protection against contact corrosion.

To ensure good bonding, the adhesive film thickness must not exceed a certain value. As applied to welded joints, this could mean a limitation of the melted area thickness. When the upper weldability limit is approached, the critical thickness of the melted area may be reached that makes bonding impossible. Thus, we can say that explosive welding "absorbs" another way of joining materials, namely their bonding by forming melted areas. The research allowed to overcome the stereotype of risk of melting during explosive welding.

It is, in particular, in case of copper-tantalum-steel composite which is used to build walls of a chemical reactor where explosive welding can be applied most successfully. The work was performed by Dynamic

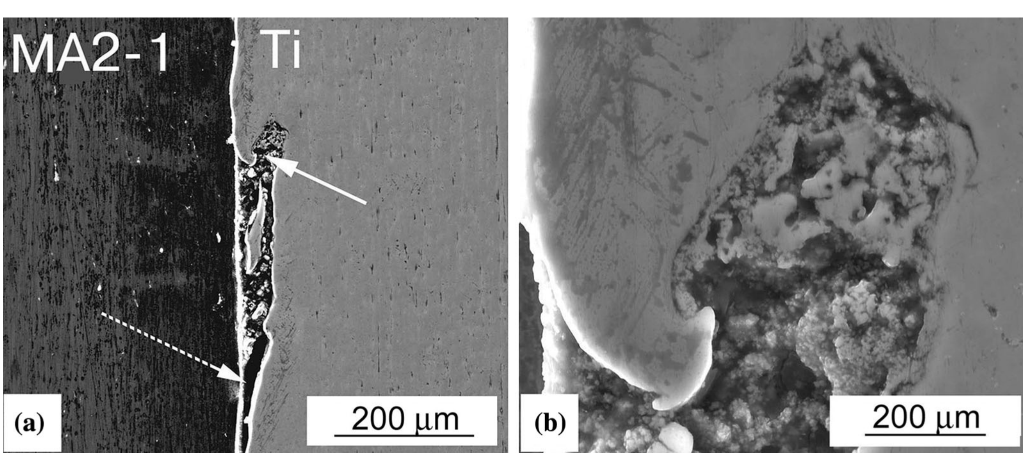

Fig. 12—Magnesium-titanium (*a*, *b*) at different magnifications, pores are visible.

Materials Corporation (USA).[22] The whole structure is based on corrosion resistance of tantalum that the inner shell of the reactor is made of. The outer shell is made of carbon steel. There is a copper layer between steel and tantalum. The tantalum-copper joint inside the reactor wall is the ($\mathbf{C}_w$) joint with a wavy interface that was repeatedly mentioned above.

Without going into details, we present here the conclusions from the analysis of the reasons for the stability of the walls of such a reactor. Due to the lack of mutual solubility of copper and tantalum, the local melted zone cannot be a true solution. For the same reason there is no diffusion here and intermetallic reactions are impossible. As a result this zone is solidified colloidal solution of tantalum in copper. Because of the high melting temperature of tantalum 3269 K (2996 °C), the colloidal solution cannot form an emulsion, and therefore there is no danger of the separation.

Thus, the lack of mutual solubility of copper and tantalum prevents the formation of intermetallic compounds, while formation of dispersion strengthened suspension in the course of melting and subsequent solidification ensures high quality and stability of the chemical reactor walls containing copper-tantalum welded joints.

VIII. CONCLUSIONS

1. The relation between local melting and GF was established. GF involves, in the first place, formation and flying away of particles. GF is to a certain extent similar to fragmentation in case of a usual explosion but occurs in the presence of a barrier. Flying away of particles can induce melting. Due to the large total area of the particles, friction between the particles and the barrier may lead to local heating sufficient for melting.
2. It was found that the particles in the melted zone are rather smooth and elongate, whereas particles that failed to fly away are indented. This is because flying away of smooth particles is an easier process than that of indented ones. Therefore smooth particles fly away, while indented ones remain on the edge of the refractory phase.
3. The relations between typical temperatures determining the conditions for the formation of microheterogeneous structures have been obtained. These structures are solidified colloidal solutions of various types: emulsions, suspensions, or foams. Exposure to solidified emulsion threatens joint continuity due to possible separation, while exposure to solidified foam is risky due to the possible porosity of the interface. On the contrary, suspension in which the dispersion medium consists of the melted (and then solidified) phase and the dispersed phase is made up of particles of the refractory phase which is not melted can strengthen the joint.
4. The fractal approach was proposed for describing the structure in the transition zone of welded joints. Various types of fractals were found and their dimensions were calculated. It is islands of different colors that inevitably occur in case of interpenetration of different materials in the process of explosive welding. Relation between the fractal dimensions and adhesion between different materials was analyzed.
5. The reasons for stability of the chemical reactor shell containing copper-tantalum junction with wavy interface were established. The lack of mutual solubility of copper and tantalum prevents the formation of intermetallic compounds. Because of the high melting temperature of tantalum, colloidal solution formed in the process of local melting of copper cannot be an emulsion. This results in local melted zones filled with suspension to be randomly scattered along the wavy interface. The suspension consists of solidified copper matrix which is strengthened with dispersed micron tantalum particles.

ACKNOWLEDGMENTS

Electron microscopic studies were performed at the Center for Collective Use of Electron Microscopy of the Ural Division of the Russian Academy of Sciences. The study was funded through a grant from the Russian Science Foundation (Project No. 14-29-00158).

REFERENCES

1. A.A. Deribas: *High Press. Res.*, 1989, vol. 1, pp. 365–76.
2. J.F. Lancaster: *Metallurgy of Welding*, 6th ed., Abington Publishing, Abington, 1999, p. 446.
3. V.I. Lysak and S.V. Kuzmin: *J. Mater. Process. Technol.*, 2012, vol. 212, pp. 150–56.
4. B.A. Greenberg, M.A. Ivanov, V.V. Rybin, O.A. Elkina, O.V. Antonova, A.M. Patselov, A.V. Inozemtsev, A.V. Plotnikov, A.Yu. Volkova, and Yu.P. Besshaposhnikov: *Mater. Charact.*, 2013, vol. 75, pp. 51–62.
5. B.A. Greenberg, M.A. Ivanov, A.M. Patselov, and Yu.P. Besshaposhnikov: *AASRI Procedia*, vol. 3d, Elsevier, Oxford, 2012, p. 66.
6. N.F. Mott: *Proc. R. Soc. Lond. Ser. A.*, 1947, vol. 189, pp. 300–08.
7. D. Grady: *Fragmentation of Rings and Shells. The Legacy of N.F. Mott*, Springer, Berlin, 2006, p. 376.
8. B.A. Grinberg, M.A. Ivanov, V.V. Rybin, O.A. Elkina, A.M. Patselov, O.V. Antonova, A.V. Inozemtsev, and T.P. Tolmachev: *Russ. Metall.*, 2013, vol. 10, pp. 727–37.
9. V.V. Rybin, B.A. Grinberg, M.A. Ivanov, S.V. Kuz'min, V.I. Lysak, O.A. Elkina, A.M. Patselov, A.V. Inozemtsev, O.V. Antonova, and V.E. Kozhevnikov: *Russ. Metall.*, 2011, vol. 10, pp. 1008–15.
10. B.A. Grinberg, M.A. Ivanov, V.V. Rybin, S.V. Kuz'min, V.I. Lysak, O.A. Elkina, A.M. Patselov, O.V. Antonova, and A.V. Inozemtsev: *Russ. Metall.*, 2011, vol. 10, pp. 1016–25.
11. V.V. Rybin, B.A. Greenberg, M.A. Ivanov, A.M. Patselov, O.V. Antonova, O.A. Elkina, A.V. Inozemtsev, and G.A. Salishchev: *J. Nanosci. Nanotechnol.*, 2011, vol. 11, pp. 8885–95.
12. B.A. Greenberg, A.V. Inozemtsev, O.V. Antonova, O.A. Elkina, A.M. Patselov, M.A. Ivanov, V.V. Rybin, S.V. Kuz'min, V.I. Lysak, and V.E. Kozhevnikov: *Phys. Met. Metall.*, 2012, vol. 113, pp. 176–89.

13. B.A. Greenberg, O.A. Elkina, A.M. Patselov, O.V. Antonova, A.V. Inozemtsev, M.A. Ivanov, V.V. Rybin, G.A. Salishchev, and V.E. Kozhevnikov: *Russ. Metall.*, 2012, vol. 10, pp. 913–20.
14. B.A. Greenberg, O.A. Elkina, A.M. Patselov, A.V. Inozemtsev, A.V. Plotnikov, A.Yu. Volkova, M.A. Ivanov, V.V. Rybin, and Yu.P. Besshaposhnikov: *Paton Weld. J.*, 2012, vol. 9, pp. 12 19.
15. M.S. Pushkin, A.V. Inozemtsev, and B.A. Greenberg: *Abstracts of International Conference: Zababakhin Scientific Talks, Snezhinsk, Russia*, 2014, p. 223.
16. B. Mandelbrot: *The Fractal Geometry of Nature*, Henry Holt and Company, New York, 1983, p. 468.
17. J. Feder: *Fractals*, Springer, Berlin, 1988, p. 283.
18. K.S. Birdi: *Handbook of Surface and Colloid Chemistry*, 3rd ed., CRC Press, Boca Raton, 2008, p. 756.
19. B.A. Greenberg, M.A. Ivanov, V.V. Rybin, O.A. Elkina, A.V. Inozemtsev, A.Yu. Volkova, S.V. Kuz'min, and V.I. Lysak: *Phys. Met. Metall.*, 2012, vol. 113, pp. 1099–1110.
20. F. Czerwinski, ed.: *Magnesium Alloys-Design, Processing and Properties*, In Tech, Rijeka, Croatia, 2011, p. 526.
21. A.V. Pocius: *Adhesion and Adhesives Technology*, 2nd ed., Hanser Publishers, Munich, 2002, p. 373.
22. D. Frey and J. Banker: *Proceedings of Corrosion Solutions Conference 2003*, Wah Chang, 2003, p. 163.